COMPARISON OF DRYOUT POWER DATA BETWEEN CANFLEX MK-V AND CANFLEX MK-IV BUNDLE STRINGS IN UNCREPT AND CREPT CHANNELS

JI SU JUN* and L.K.H. LEUNG[1]
Korea Atomic Energy Research Institute
150, Deokjin-dong, Yuseong-gu, Daejeon 305-353, Korea
[1]Atomic Energy of Canada Limited
Chalk River, Ontario, K0J 1J0, Canada
*Corresponding author. E-mail : junjisu@kaeri.re.kr

Received January 21, 2005
Accepted for Publication June 29, 2005

The CANFLEX Mk-V bundle is designed to improve upon the critical heat flux (CHF) characteristics of the CANFLEX Mk-IV bundle. The main difference between these two bundles is an increase in bearing pad height of about 0.3 mm in the CANFLEX Mk-V bundle. This change in bearing pad height leads to an increase in gap flow at the bottom of the bundle, primarily eliminating the localized narrow-gap effect that limits the CHF of the CANFLEX Mk-IV bundle. The objective of this paper is to examine the effects of bearing pad height and pressure tube creep on the sheath-temperature distribution, dryout power, and dryout location, as observed from full-scale bundle tests, between CANFLEX Mk-IV and Mk-V bundles in uncrept and crept channels. A comparison of surface-temperature differences between the top and bottom elements of the bundles showed that increasing the bearing pad height has led to a more homogeneous enthalpy distribution in subchannels of the bundle. Initial dryout locations of the CANFLEX Mk-V bundle were mainly observed at the mid-spacer plane of either the 10th (about 80%) or 11th (20%) bundle in the 12-bundle string, as compared to the mid-spacer and downstream-button planes for the CANFLEX Mk-IV bundle. Dryout power and boiling-length-average (BLA) CHF values exhibit consistent trends and little scatter with varying flow conditions for both types of CANFLEX bundles in uncrept and crept channels. An increase in pressure tube creep has led to a reduction in dryout power (about 20% for the 3.3% crept channel and 27% for the 5.1% crept channel as compared to dryout powers for the uncrept channel). Increasing the bearing pad height of the CANFLEX bundle has led to an increase in the dryout power. Overall, the dryout power of the CANFLEX Mk-V bundle is 7 to 10% higher than that of the CANFLEX Mk-IV bundle at the inlet temperature range of interest (i.e., between 243 and 290°C).

KEYWORDS : Full-Scale Bundle Test, Bearing Pad Height, CANFLEX Bundle, Dryout Power, Critical Heat Flux, Pressure Tube Creep

1. INTRODUCTION

The CANFLEX (CANDU Flexible) fuel bundle has been jointly developed since 1991 by the Korea Atomic Energy Research Institute (KAERI) and Atomic Energy of Canada Limited (AECL) as an advanced nuclear fuel for a pressurized heavy water reactor. It is composed of 43 dual-sized rods (8 rods with large diameter and 35 rods with small diameter). Heat-transfer enhancing appendages (referred to as buttons) are attached to the surface of the elements. Figure 1 shows a cross-sectional view and picture of the CANFLEX bundle (half length). As compared to the CANDU 37-element bundle, the reduction in element diameter reduces the outer-element power [1] and the introduction of buttons improves the thermal hydraulic performance of the CANFLEX bundle. The development of a CANFLEX bundle with 1.4 mm bearing pad (BP) (called as low BP or CANFLEX Mk-IV) has been completed. Demonstration irradiation (DI) programs of 24 CANFLEX Mk-IV bundles with natural uranium fuel were carried out from September 1998 to August 2000 at the Point Lepreau Generating Station (PLGS) in Canada [2] and from July 2002 to February 2004 at the Wolsong-1 reactor in Korea [3].

Critical heat flux (CHF) tests, jointly funded by AECL and KAERI, were performed at Stern Laboratories (SL) in Hamilton, Canada, to obtain thermalhydraulic data for licensing submissions of the CANFLEX Mk-IV bundle

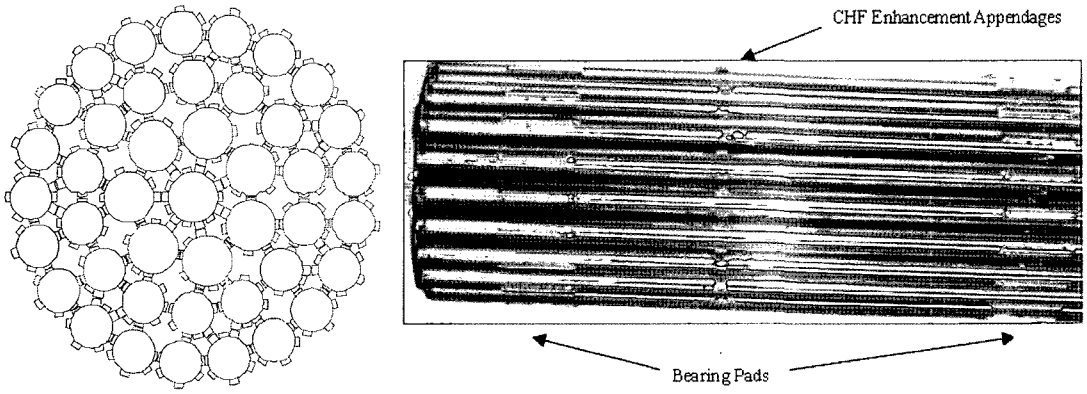

Fig. 1. Picture of the CANFLEX Fuel Bundle

[4,5]. The test section simulated a full-scale aligned CANFLEX Mk-IV bundle string equipped with junctions and appendages (spacers, buttons, and bearing pads). It had non-uniform radial (simulating fresh natural uranium fuel) and axial (downstream skewed-cosine shape) heat flux distributions. The bundle string simulator was tested in three different channels of no creep (uniform), 3.3% maximum creep, and 5.1% maximum creep. Observations from these full-scale bundle tests indicated that elements at the bottom portion of the bundle are the preferential dryout location [6] and the sheath temperature of elements at the bottom portion is higher than that at the top portion of the bundle. This appears to suggest that a significant flow imbalance is present between the top and bottom portions. Furthermore, the imbalance appears to increase with increasing channel creep.

Hence, a minor bundle-design modification was introduced in order to improve the CHF characteristics of the CANFLEX bundle. The BP height of the bundle has been increased from 1.4 mm to 1.7 mm. This change is designed to increase the gap flow at the bottom portion of the bundle (where dryout occurs) and decrease the enthalpy imbalance between the top and bottom portions of the bundle by reducing the bundle eccentricity in the horizontal channel. The modified bundle design is referred to as the CANFLEX Mk-V bundle. Additional CHF tests were performed for the CANFLEX Mk-V bundle by attaching thin metal shims to BPs of the CANFLEX Mk-IV bundle-string simulator [7].

This paper analyzes the dryout power and the CHF data of the CANFLEX Mk-V bundle and examines the effects of bearing pad height and pressure tube creep on the enthalpy distribution, the dryout power, and the dryout location of the CANFLEX Mk-V bundle. Furthermore, the enhancement in dryout power of the CANFLEX Mk-V bundle compared to that of the CANFLEX Mk-IV bundle is quantitatively assessed. The procedure of a full-scale CHF test is also briefly explained so as to provide an understanding of how to obtain the dryout power data of the CANFLEX fuel bundle. The effects of bearing pad height and pressure tube creep on the enthalpy distribution are examined by using the bundle cross-section profile map, which is generated from the element surface temperature data under single-phase flow conditions. The dryout locations are classified by the percentage number of data at the front of the appendages where dryout occurs. Data trends of the measured dryout power are examined by the variations of the test loop control parameters (inlet temperature, mass flow rate, and outlet pressure). The boiling-length-average (BLA) CHF is also examined at various local flow conditions (quality, mass flux, and pressure). The BLA CHF is used for the analysis of the dryout power data, because the local CHF is highly dependent on dryout location, and thus shows significant data scattering. The effects of bearing pad height and pressure tube creep on the dryout power are quantified by classifying the relevant data.

2. FULL-SCALE WATER CHF TESTS

Thirteen series of high-pressure steam-water tests were carried out to obtain steady-state CHF data for CANFLEX bundles in uncrept and crept channels at SL, where similar tests were performed for a 37-element bundle [8]. The chronology of the CANFLEX water CHF test series is shown in Table 1, which presents the pressure tube creep, the test name, the order of test, the bearing pad height, and the number of dryout power data for each series. The tests for the CANFLEX Mk-IV bundle with low bearing pads (BP: 1.4 mm) were first conducted in 5.1% crept (C1), 3.3% crept (C2) and uncrept (R1) pressure tubes, respectively, from February 1999 to June 1999. Tests (B1, B2, B3, B4) for CANFLEX Mk-V with high BP (1.7 mm or 1.8 mm) as well as repeatability and reproducibility

Table 1. The Chronology of the CANFLEX Water CHF Test Series

Creep	Series Name	Date	Test Order	No. of Dryout Power Data	Nominal Bearing Pad Height	Bundle Restraining Top Hats
0%	R1	June-1999	3	85	1.40 mm	No
	R1a	Nov.-1999	4	52	1.40 mm	No
	R2	Feb.-2000	7	51	1.35 mm	Yes
	B1	Mar.-2000	8	85	1.80 mm	Yes
	B5	Jan.-2001	13	100	1.70 mm	Yes
3.3%	C2	May-1999	2	107	1.40 mm	No
	B4	June-2000	12	58	1.70 mm	Yes
5.1%	C1	Mar.-1999	1	106	1.40 mm	No
	C1a	Nov.-1999	5	26	1.40 mm	No
	C3	Jan.-2000	6	55	1.35 mm	No
	C4	Apr.-2000	10	33	1.32 mm	Yes
	B2	Mar.-2000	9	49	1.80 mm	Yes
	B3	May-2000	11	57	1.70 mm	Yes

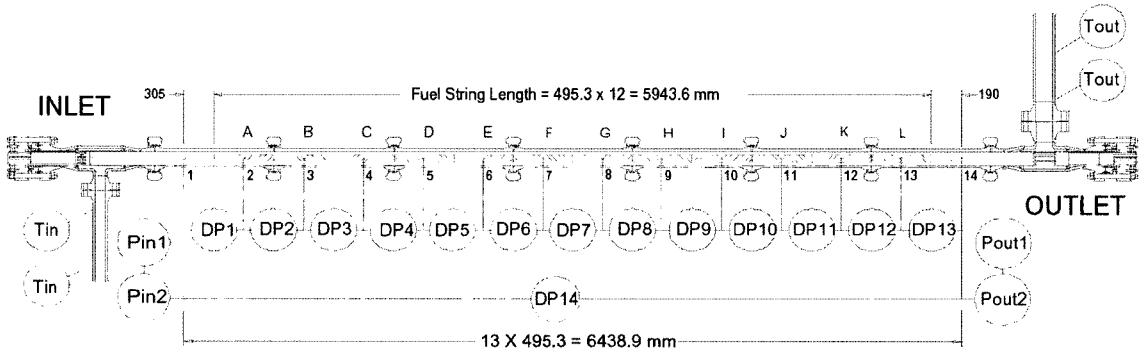

(a) Test Section

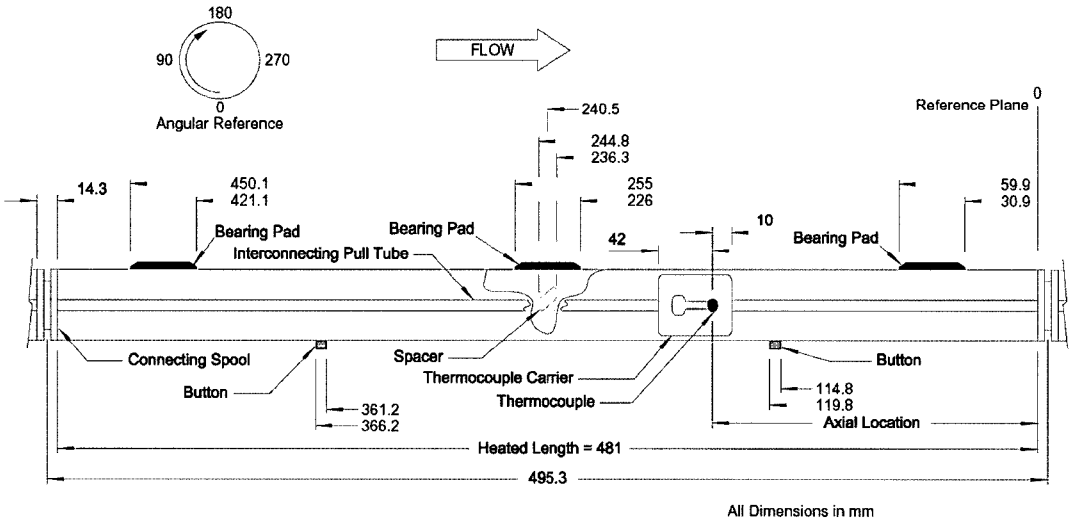

(b) T/C Carrier Installed Inside a Heater Tube

Fig. 2. Test Section Instrumentation for the Full-Scale Bundle Water CHF Test

tests for a low BP bundle (R1a, C1a, C3, R2, C4) were subsequently conducted from November 1999 to June 2000. The last experiment was performed for a 1.7 mm BP height bundle (B5) in the uncrept tube in January 2001. In the case of the C3, R2, and C4 series, the height of the bearing pads (1.35 mm, 1.35 mm, and 1.32 mm) was slightly lower than the designed value of 1.4 mm. This discrepancy may have been caused by wear during the experiments. The bundle string was equipped with junctions and appendages (spacers, buttons, and bearing pads) and was heated by a DC current. The transformation to the CANFLEX Mk-V design was achieved by attaching thin metal shims to the bearing pads of the CANFLEX Mk-IV bundle simulator. In addition, top hats spacers were fitted over the bearing pads on three top elements so as to prevent any possible movement of the bundle string in the flow tube during testing.

Figure 2 shows the test section instrumentation in detail. Loop conditions at both the inlet and outlet ends of the bundle string are monitored with differential-pressure cells and thermocouples (T/C). In addition, pressure taps are installed at various locations along the bundle string to obtain the pressure drop data. Spring-loaded thermocouples mounted on sliding T/C carriers are installed inside all 43 heater tubes of the five downstream bundles (indicated as H, I, J, K, and L in Figure 2), where dryout preferentially occurs (axial distance beyond 3.5 m). The thermocouples are moved axially and rotated so as to obtain the surface temperature at various locations of each heater tube. During the CHF test, the power is raised incrementally while maintaining constant outlet pressure, inlet temperature, and flow rate. A continuous scan of all the test section thermocouples is carried out in order to obtain the first indication of dryout. Initial dryout is first indicated when the standard deviation of any temperature signal exceeds 0.5°C, or when the calculated external surface temperature is more than 10°C above the average for all the thermocouples.

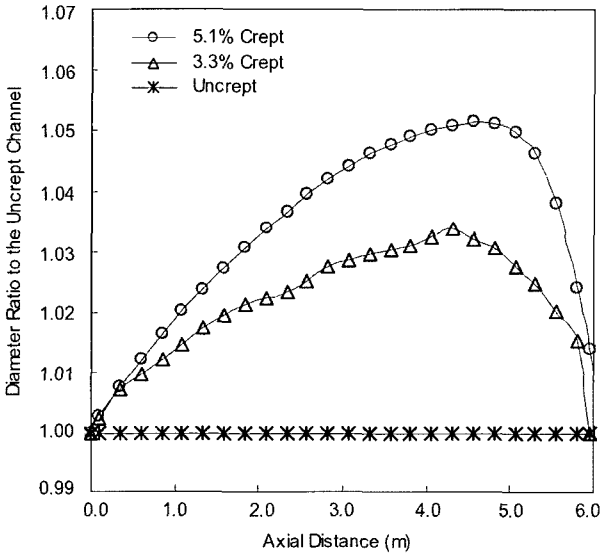

Fig. 3. Axial Variations of the Inside Diameter in the Crept Channels

The test fuel bundle string has an axially and radially non-uniform heat flux profile. The bundle string has an axial heat flux distribution (AFD) of a downstream skewed-cosine profile, where the peak ratio is 1.6204, and it is located at a 3.8 m axial distance. This distribution has been anticipated to provide a lower dryout power than the reference symmetric-cosine profile. The radial heat flux distribution (RFD) simulates the profile with fresh uranium fuel, where the relative ring power ratio to the bundle power is 1.034, 1.081, 0.873, and 1.056 for the elements in the outer ring, intermediate ring, inner ring, and centre rod, respectively. The bundle string is installed into three different ceramic flow tubes (uncrept, 3.3% crept, and 5.1% crept), as shown in Figure 3. The maximum diametral creep is located 4.3 m from the inlet for the 3.3% crept channel, and 4.8 m from the inlet for the 5.1% crept channel. These profiles simulate the pressure tube creep deformation during the plant operating life time. The test flow conditions cover a wide range of outlet pressure from 6 to 11 MPa, mass flow rate from 7 to 29 kg/s, and inlet temperature from 200 to 290°C.

3. ANALYSIS OF TEST DATA

3.1 Subchannel Flow Imbalance

In the CANFLEX Mk-IV bundle [5,6], the dryout power decreased rapidly with an increase in the pressure tube creep. Dryout occurred mostly at the bottom elements of the outer ring. This indicates that CHF is highly dependent on the pressure tube creep and heat transfer rate at the bottom portion of the channel. A slight increase (about 0.3 mm) in the bearing pad height for the CANFLEX Mk-V bundle is designed so as to increase the gap flow at the bottom of the bundle and to decrease the enthalpy imbalance between the top and bottom portions of the bundle by reducing the bundle eccentricity in the horizontal channel. The bundle eccentricity [9] in the uncrept pressure tube becomes 0.084, 0.057, and 0.046 with respect to bearing pad heights of 1.4 mm, 1.7 mm, and 1.8 mm, respectively. The decrease in the eccentricity would move the bundle closer to the center of the channel and increase the subchannel sizes at the bottom portion of the bundle. As a consequence, the flow rate is increased in the expanded subchannels at the bottom of the bundle. This results in more efficient cooling to the bottom elements.

Heat balance tests were carried out regularly during the experiment to check the performance of the test loop and instrumentation. In conjunction with most heat balance tests, temperature profile scan tests were performed to record the element surface temperature by rotating the thermocouples at the mid-spacer plane of the bundle (at

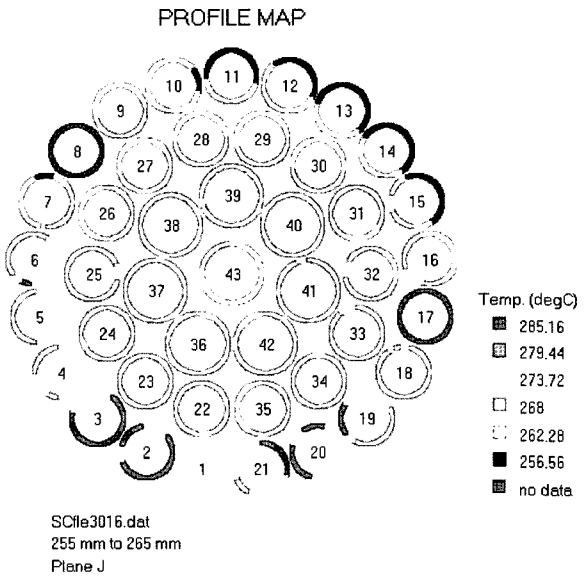

Fig. 4. Surface Temperature Scan Profile Map

the half of the bundle). Figure 4 is an example of a bundle cross-section profile map generated from these temperature data. It shows the surface temperature distribution and provides an indication of the flow distribution in the bundle subchannels.

The effects of bearing pad height on the temperature distribution are examined by comparing the profile maps for the uncrept channel under the same single-phase flow conditions with an inlet temperature of 180 °C, a flow rate of 25 kg/s, an outlet pressure of 9 MPa, and a power of 9 MW. It is observed that the temperature difference between the bottom elements and the top elements is rapidly reduced from 42 °C (1.4 mm) to 35 °C (1.7 mm) and 29 °C (1.8 mm) as the height of the bearing pad increases. In addition, it is shown that the hottest temperature of the bottom elements is decreased from 291°C (1.4 mm) to 288 °C (1.7 mm) and 285 °C (1.8 mm) as the height of the bearing pad increases. This improvement of heat transfer for the CANFLEX Mk-V bundle results in a more homogeneous sheath temperature of the elements at the center portion of the channel.

The effects of pressure tube creep on the temperature distribution are also examined by comparing the profile maps for the various crept channels (uncrept, 3.3%, and 5.1% crept, respectively) under the same single-phase flow conditions of an inlet temperature of 180 °C, an outlet pressure of 9 MPa, a flow rate of 13.5 kg/s, and a power of 2 MW. It is observed that the temperature difference between the bottom elements and the top elements of the 1.7 mm bearing pad bundle increases from 8 °C for the uncrept channel to 23 °C for the 3.3% crept channel and 28 °C for the 5.1% crept channel. In addition, the maximum sheath temperature at the bottom elements rises with the channel creep (226 °C for the uncrept channel, 236 °C for the 3.3% crept channel, and 243 °C for the 5.1% crept channel). The increase in the temperature difference and the maximum sheath temperature is caused by the increased bypassing flow through the gap between the top elements and the pressure tube. For the 1.4 mm bearing pad bundle, the creep effect on the temperature distributions is similar to that of the 1.7 mm bearing pad bundle, but the increase in the temperature difference and the maximum sheath temperature are slightly greater than those of the 1.7 mm bearing pad bundle.

3.2 Dryout Location

The five downstream bundles among the total 12 bundles are designated H, I, J, K, and L bundle, as shown in Figure 2. Sliding T/C carriers are installed into these bundles only because dryout is anticipated to occur downstream of the bundle string. The dryout location of the bundle string geometry with non-uniform AFD and RFD is dependent on the flow conditions, while the dryout for a simple geometry (such as a tube) with uniform AFD occurs at a fixed location near the outlet. Dryout occurs preferentially at the front of appendages, i.e. bearing pads and buttons. Hence, five T/C locations are selected in this study, i.e. 17 mm, 65 mm, 125 mm, 250 mm, and 260 mm from the downstream endplate (see Figure 2b). Figure 5 shows the distribution of the axial dryout location for the test data in the uncrept (R1, B1 and B5) channel of the low bearing pad and high bearing pad bundles. Similar figures are obtained by test data in the 3.3% crept (C2, B4) and the 5.1% crept (C1, B2 and B3) channels, respectively. For the low bearing pad bundles, the initial dryout is mainly located at the mid-

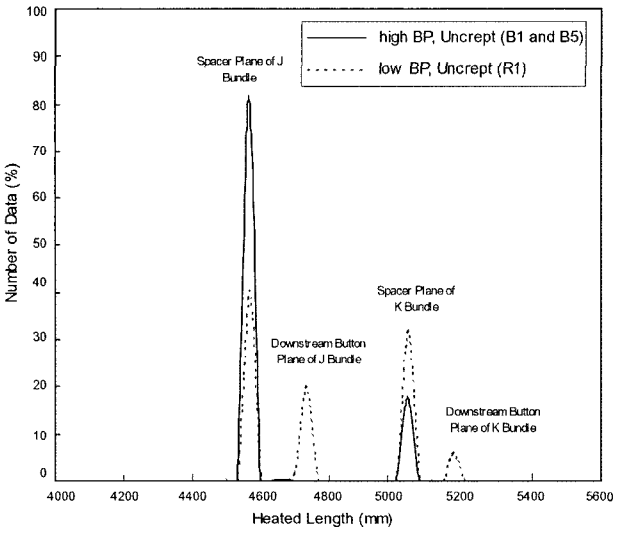

Fig. 5. Axial Dryout Locations Observed in the Uncrept Channel

spacer plane (at T/C location of 250 mm), the downstream button plane (at 125 mm), and the bearing pad plane (at 260 and 65 mm) of the J and K bundles. Some dryout occurs at the downstream endplate (at 17 mm) of the J bundle in the 5.1% crept channel. By increasing the pressure tube creep, the dryout locations are moved from the J bundle to the K bundle. For example, the percentage number of data on the mid-spacer plane and downstream button plane of the K bundle is 32% and 6% in the uncrept tube, 37% and 15% in the 3.3% crept tube, and 33% and 28% in the 5.1% crept tube, respectively. On the other hand, the majority of the initial dryout for the high bearing pad bundles occur at the mid-spacer plane (81%, 79%, and 74% for the uncrept, 3.3% crept, and 5.1% crept channels, respectively) of the J bundle and the mid-spacer plane (18%, 21%, and 22% for the uncrept, 3.3% crept, and 5.1% crept channels, respectively) of the K bundle. Some dryout locations are observed at the downstream endplate (3%) of the J bundle in the 5.1% crept channel. By increasing the pressure tube creep, the dryout location tends to shift to the downstream end. For the low bearing pad bundles with top hats spacers (R2 and C4), the majority of the dryout also occurs at the J bundle.

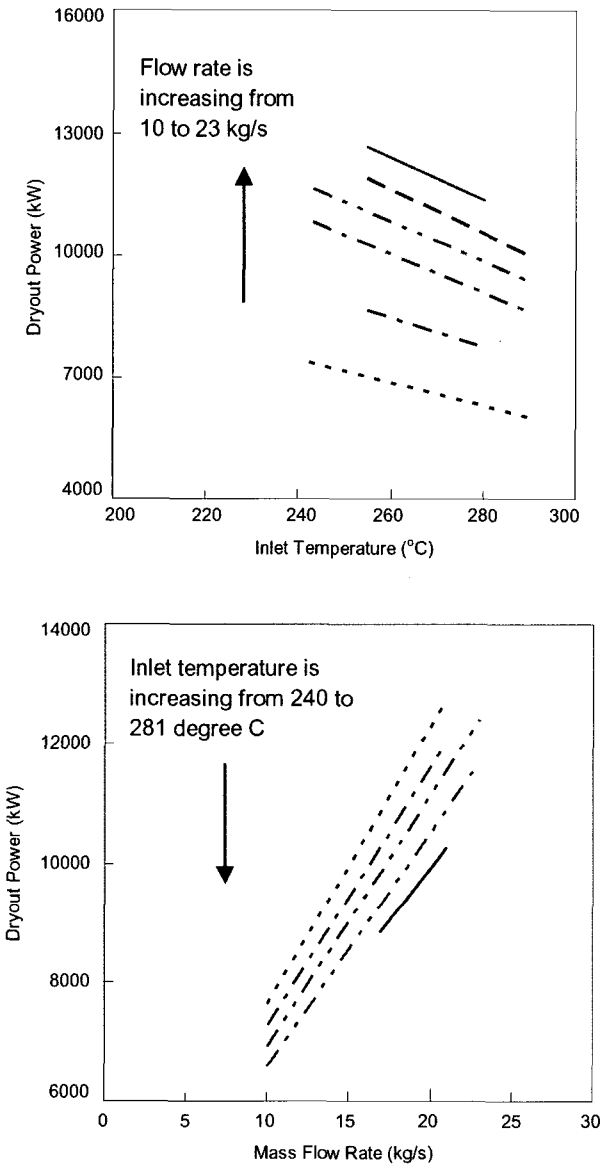

Fig. 6. Effects of Subcooling and Mass Flow Rate on the Dryout Power

3.3 Data Trend of Dryout Power and CHF

In the system flow condition approach, the measured dryout powers are examined by varying the test loop control parameters (inlet temperature, mass flow rate, and outlet pressure). This approach is known to show more consistency with a small data scattering, and to be less affected by other parameters such as axial power profile and dryout location. Basically, dryout is a local phenomenon, mainly dependent on the flow conditions at the dryout locations. Figure 6 shows the effects of the inlet temperature (subcooling) and mass flow rate on the dryout power in the high bearing pad bundles (B1 data) at 11 MPa and 9 MPa, respectively. The dryout power increases with an increasing flow rate and decreases with an increasing inlet temperature. The effect of outlet pressure on the dryout power is exhibited in Figure 7 for the 1.7 mm bearing pad bundles in a 3.3% crept tube (B4 data) at mass flow rates of 17 kg/s. This clearly shows an increasing trend of dryout power with pressure; however, the impact of pressure is less significant than that of flow rate and inlet temperature.

In the constant dryout condition approach, the calcula-

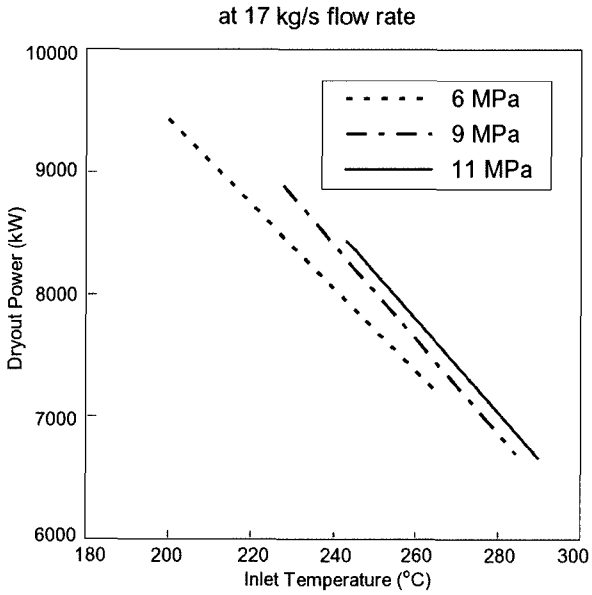

Fig. 7. Effect of Outlet Pressure on the Dryout Power

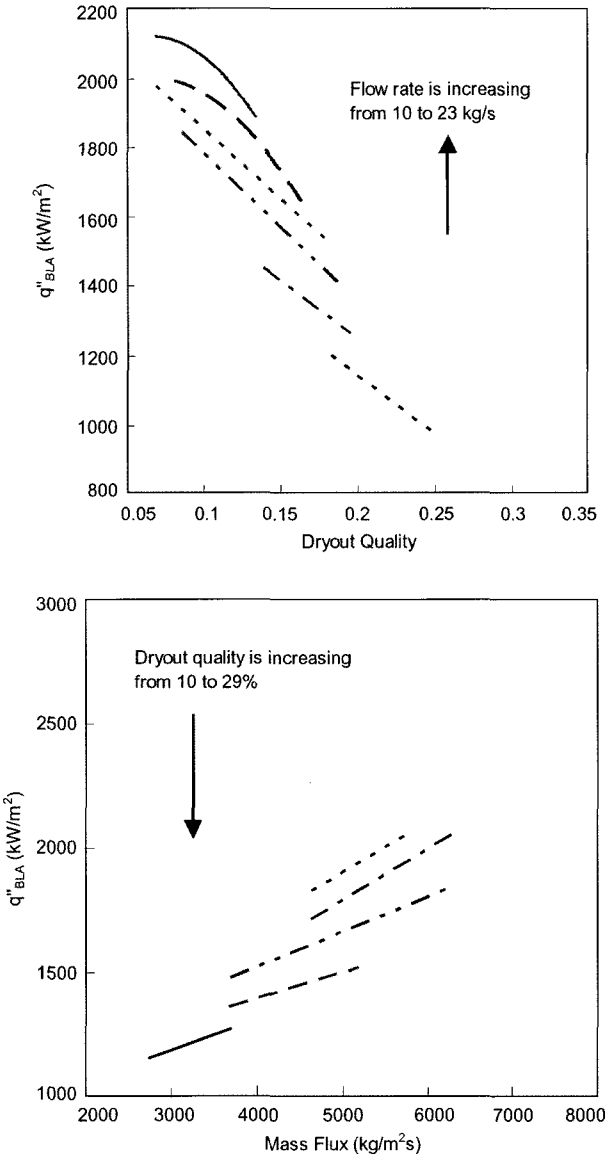

Fig. 8. Effects of Critical Quality and Mass Flux on the BLA CHF

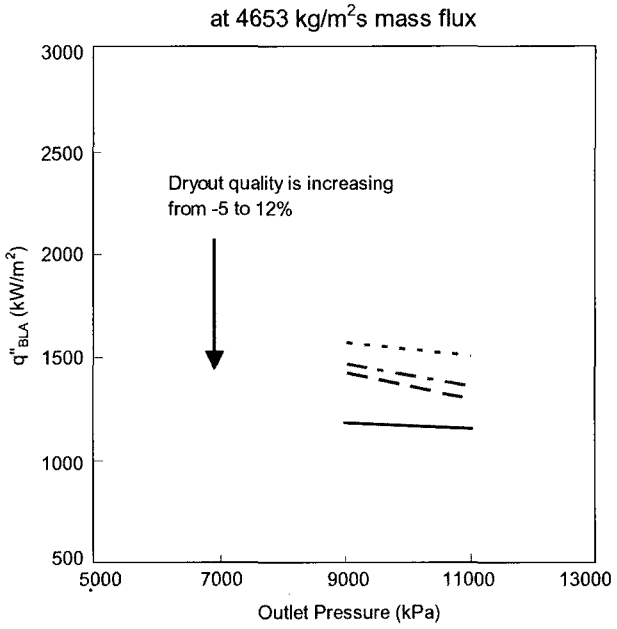

Fig. 9. Effect of Outlet Pressure on the BLA CHF

ted CHF values are examined by varying the local flow conditions at the dryout location (quality, mass flux, and pressure). This study uses the parameter of BLA CHF instead of the local CHF, because the local CHF is very dependent on the dryout location and thus shows significant data scattering. BLA CHF is defined as the sum of the dryout power over a heated area from the location of the onset of significant void (OSV) to the location of the dryout. The BLA concept was introduced to account for the AFD effect on CHF. The BLA CHF shows more consistency and less data scattering with the critical quality than the local CHF in uncrept and crept channels [7]. For the CANDU fuel bundle, the initiation of boiling is defined at the OSV point instead of at the saturation point due to the enthalpy imbalance among the subchannels in the bundle. The OSV points were obtained at the transition location from the single-phase to two-phase flow region with SL pressure drop measurements [9].

Figure 8 shows the effects of critical quality and mass flux on the BLA CHF in the high bearing pad bundles at pressures of 11 MPa and 9 MPa, respectively. The BLA CHF decreases with increasing dryout quality and it increases with increasing mass flux. This trend is consistent with the effects of subcooling and mass flow rate on the dryout power, as previously shown in Figure 6. However, the data scattering becomes larger at low flow rate (10 kg/s and 13.5 kg/s) and high quality conditions. The BLA CHF depends more strongly on the dryout locations than the dryout power does. As shown in Figure 8, a smooth variation of BLA CHF with the dryout quality is observed at the low quality region for a high flow rate (21 kg/s and 23 kg/s) and 11 MPa of outlet pressure for the 1.8 mm bearing pad bundle (B1 Data) in the uncrept channel. At the same dryout quality, the BLA CHF increases with increasing mass flux. The data trends are consistent for both pressures, i.e. 9 MPa and 11 MPa. However, the data scattering of BLA CHF increases at 6 MPa pressure. The local CHF data has higher data scattering than the BLA CHF as the pressure tube creep increases. Figure 9 shows the effect of outlet pressure on BLA CHF at a constant mass flux and dryout quality for the 1.7 mm bearing pad bundles in the 5.1% crept (B3 Data) channel. The BLA CHF decreases slightly with increasing pressure. This trend differs from that shown in Figure 7 based on the dryout power. This

difference is caused by the change of quality as the pressure varies.

3.4 Increase in Dryout Power

The impacts of the bearing pad height on the dryout power are examined using all the test series data. The dryout powers for the uncrept channel at 11 MPa outlet pressure and 268 °C inlet temperature and different bearing pad heights are classified and shown in Figure 10. This figure clealry shows that the dryout power in the high bearing pad bundle is greater than that in the low bearing pad bundle. Based on these results, the relative increase in the dryout power with respect to the 1.4 mm bearing pad bundle is obtained and shown in Figure 11. For the test conditions of 11 MPa outlet pressure and 17 kg/s and 21 kg/s mass flow rates, the dryout powers in the bundles with 1.7 mm and 1.8 mm bearing pad heights are consistently higher by about 5%~11% and 6%~12%, respectively, than those of the 1.4 mm bearing pad bundle at an inlet temperature range of 243 °C~290 °C. The amount of increase in dryout power for the high bearing pad bundle gradually decreases with increasing inlet temperature. In the middle range of the inlet temperature, the average gain of the dryout power for the high bearing pad bundles (1.7 mm and 1.8 mm) is about 7% to 10% with respect to the low bearing pad bundles (1.4 mm, 1.35 mm, and 1.32 mm). For the 1.35 mm and 1.32 mm bearing pad bundles, a reduction in the dryout power is observed when compared to the 1.4 mm bearing pad bundles (about 5% maximum). The data trend, however, is not consistent. For the data at 9 MPa and 6 MPa outlet pressure, the dryout power gain is similar to that at 11 MPa outlet pressure, but the gain for the 1.7 mm bearing pad bundle becomes small (less than 2%) at the higher temperatures (greater than 273 °C at 9 MPa and 265 °C at 6 MPa). On the other hand, the dryout power gain for the 1.8 mm bearing pad bundle

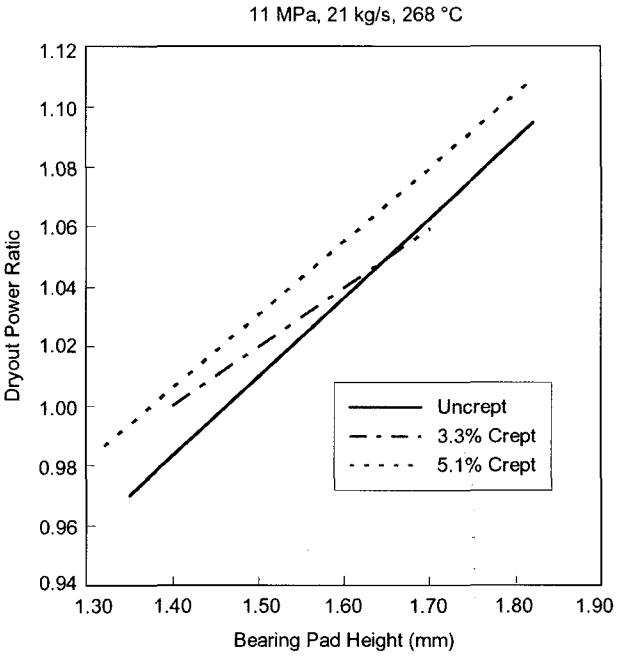

Fig. 11. Relative Dryout Power Ratio with Respect to the 1.4 mm BP Bundle

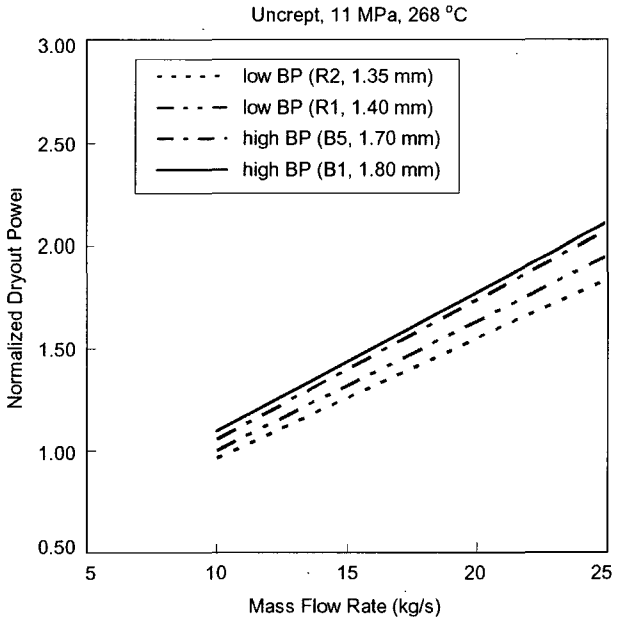

Fig. 10. Effect of BP Height on the Dryout Power

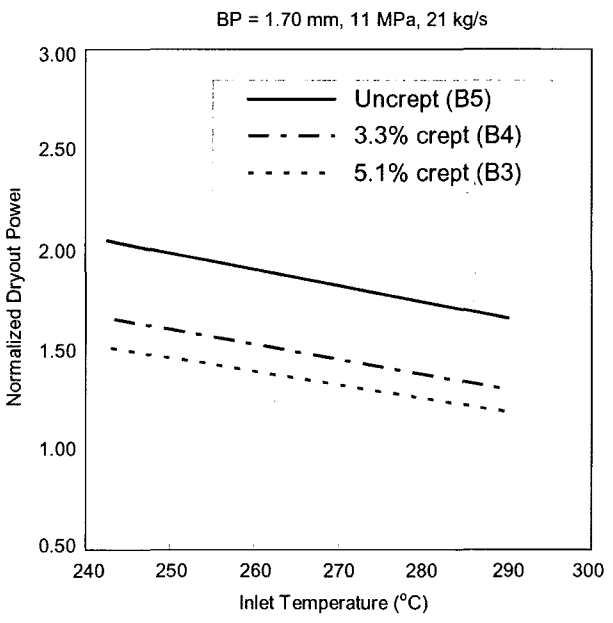

Fig. 12. Effect of Pressure Tube Creep on the Dryout Power

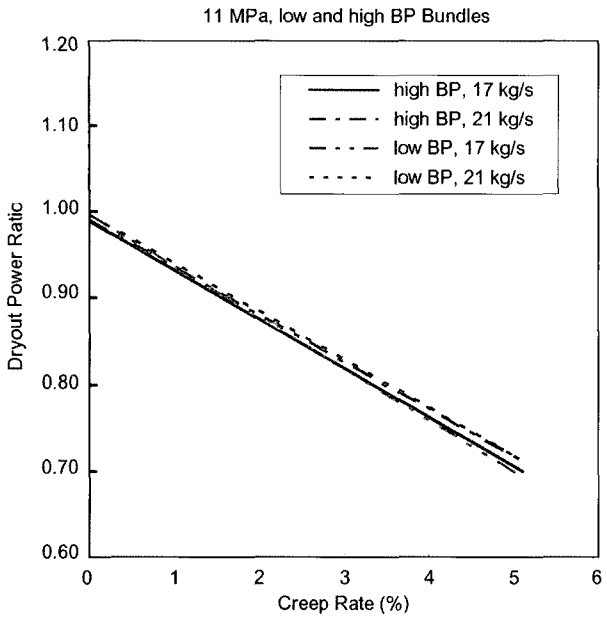

Fig. 13. Relative Dryout Power Ratio with Respect to the Uncrept Channel

remains high at high temperature conditions (4% at 9 MPa and 5% at 6 MPa). The effects of the pressure tube creep on the dryout powers for both the 1.7 mm and 1.4 mm bearing pad bundles at 11 MPa outlet pressure and 21 kg/s mass flow rate are presented in Figure 12 and Figure 13. The figures clearly show that the pressure tube creep results in a rapid decrease in the dryout power. That is, the dryout power in the 3.3% crept channel and in the 5.1% crept channel is about 20% and 27% less than that in the uncrept channel, respectively. The effect of the pressure tube creep on the dryout power with respect to the uncrept channel is similar for both the low and the high bearing pad bundles.

4. CONCLUSIONS

The CANFLEX Mk-V bundle has been designed to improve upon the CHF and heat transfer of the CANFLEX Mk-IV bundle. These improvements are achieved with a simple increase of the BP height by 0.3 mm, which has led to an increase in gap flow to the bottom elements of the bundle. Full-scale CHF tests were carried out for CANFLEX Mk-V and CANFLEX Mk-IV bundles in uncrept, 3.3% crept, and 5.1% crept channels. Reductions in maximum surface temperature at the bottom elements and surface-temperature differences between the top and bottom elements were observed for bundles with high BPs at single-phase and nucleate-boiling conditions. This reflects that increasing BP height has led to increased homogeneity in enthalpy distribution among subchannels of the bundle.

Dryout locations for the CANFLEX Mk-V bundle were observed at the mid-spacer planes of the 10th (about 80%) and 11th (20%) bundles in the 12-bundle string. The dryout locations for the CANFLEX Mk-IV bundle were distributed between the mid-spacer and downstream button planes of these two bundles. Variations of dryout power measurements have been examined with respect to inlet temperature, mass flow rate, and outlet pressure. Effects of bearing pad height and pressure tube creep on dryout power have been quantified. Dryout powers of high BP bundles are greater than those of the low BP bundle. The dryout power of the CANFLEX Mk-V bundle is about 7 to 10% higher than that of the CANFLEX Mk-IV bundle in the middle range of the inlet temperature (243~290°C). However, the gain in dryout power decreases with increasing inlet temperature. The dryout power decreases with increasing pressure–tube creep; the reduction is about 20% and 27% for the 3.3% and 5.1% crept channels, respectively, as compared to the uncrept channel for both CANFLEX Mk-V and Mk-IV bundles.

The BLA CHF is introduced by averaging the dryout power over a heated area from the location of OSV to the location of dryout. Variations of BLA CHF values have been examined with respect to critical quality, mass flux, and pressure. The BLA CHF values exhibit a consistent trend with small data scatter for CANFLEX Mk-V and Mk-IV bundles in uncrept and crept channels. In general, the BLA CHF decreases with increasing dryout quality, increases with increasing mass flux, and decreases slightly with increasing pressure.

5. ACKNOWLEDGEMENTS

This work was carried out under the Nuclear Research and Development Program of MOST (Ministry of Science and Technology) in Korea, and under the JCDP (KAERI/AECL Joint CANFLEX Development Program). CANFLEX is a registered trademark of KAERI/AECL and CANDU (Canada Deuterium Uranium) is a registered trademark of AECL.

REFERENCES

[1] J.S. Jun, H.C. Suk, M.S. Cho, J.Y. Jung, C.K. Jo and C.J. Jeong, "The Design Manual of CANFLEX-NU Fuel Bundle for CANDU-6 Reactor", KAERI/TR-2576/2003(internal report), October 2003.

[2] W.W.R. Inch, H.C. Suk, "Demonstration Irradiation of CANFLEX in Pt. Lepreau", IAEA Technical Committee Meeting on Fuel Cycle Options for LWRs and HWRs, Victoria, Canada, April 1998.

[3] J.Y. Jung, J.S. Jun, M.S. Cho, H.C. Suk, S.D. Lee and H.B. Seo, "Evaluation of CANFLEX-NU Fuel Performance Irradiated in Wolsong Generation Station #1 and In-Bay Inspection", Proceedings of the KNS Spring Meeting, Korea, May 2004.

[4] G.R. Dimmick, W.W.R. Inch, J.S. Jun, H.C. Suk, G.I. Hadaller, R.A. Fortman and R.C. Hayes, "Full Scale Water CHF Testing of the CANFLEX Bundle", the 6th International Conference on CANDU Fuel, Canadian Nuclear Society, September 1999.

[5] J.S. Jun, H.C. Suk, and J.H. Park, "The Analysis of Water CHF Test Data of CANFLEX-NU Fuel Bundle", Proceedings of the KNS Spring Meeting, Korea, May 2000.

[6] J.S. Jun, H.C. Suk, and J.H. Park, "The Water CHF Tests of CANFLEX-NU Fuel Bundle in Crept Pressure Tubes", Proceedings of the KNS Spring Meeting, Korea, May 2000.

[7] L.K.H. Leung, J.S. Jun, D.E. Bullock, W.W.R. Inch and H.C. Suk, "Dryout Power in a CANFLEX Bundle String with Raised Bearing Pads", the 7th International Conference on CANDU Fuel, Canadian Nuclear Society, September 2001.

[8] R.A. Fortman, G.I. Hadaller, R.C. Hayes and F. Stern, "Heat Transfer Studies with CANDU Fuel Simulators", the 5th International Conference on Nuclear Engineering, ICONE5, 1997 May, Nice, France.

[9] L.K.H. Leung, D.C. Groeneveld, G.R. Dimmick, D.E. Bullock, and W.W. Inch, "Critical Heat Flux and Pressure Drop for a CANFLEX Bundle String Inside an Axially Non-Uniform Flow Channel", Proceedings of the 6th International Conference on CANDU Fuel, Canadian Nuclear Society, September 1999.